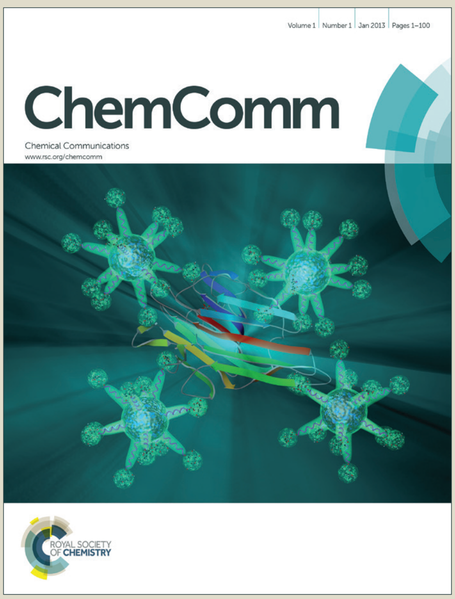
Volume 1 | Number 1 | Jan 2013 | Pages 1–100
ChemComm
Chemical Communications
www.rsc.org/chemcomm
ROYAL SOCIETY OF CHEMISTRY

Journal Name

Dynamic Article Links ►

Cite this: DOI: 10.1039/c0xx00000x

www.rsc.org/xxxxxx

ARTICLE TYPE

A new ligand skeleton for imaging applications with d/f complexes: combined lifetime imaging and high relaxivity in an Ir/Gd dyad

Atanu Jana,[a] Elizabeth Baggaley,[a] Angelo Amoroso[b] and Michael D. Ward*[a]

Received (in XXX, XXX) Xth XXXXXXXXX 20XX, Accepted Xth XXXXXXXXX 20XX

DOI: 10.1039/b000000x

A new rigid and conjugated ligand structure connecting phenanthroline and poly(amino-carboxylate) binding sites provides d/f complexes which show high potential for use in dual (luminescence + magnetic resonance) imaging and for optimisation of d→f photoinduced energy-transfer.

Phosphorescent metal complexes offer major advantages over conventional fluorescent organic molecules as the basis of luminescent probes for cell imaging.[1-3] The long luminescence lifetimes associated with triplet emission from complexes of *e.g.* Pt(II),[2a] Re(I),[2b] Ir(III),[2c] Ru(II),[2d] and lanthanides,[2e] allow simple rejection of short-lived background autofluorescence which might otherwise interfere. In addition, *variations* in luminescence lifetimes of such complexes (or 'probes') in different cellular regions, caused by the presence of different analytes such as O_2, provide the basis of the recently-developed microsecond-scale lifetime mapping techniques *phosphorescence lifetime imaging* (PLIM)[2d,3] and *time-resolved emission microscopy* (TREM).[2a,3b,3c]

In addition, the use of highly paramagnetic complexes – often of Gd(III) – for magnetic resonance imaging (MRI) is now well established.[4] Compared to luminescence-based imaging, MRI is quite complementary. Confocal microscopy offers excellent sensitivity and spatial resolution (particularly when two-photon excitation is used), but is limited in terms of tissue penetration; it is excellent for providing cellular-level detail. In contrast, MRI is capable of imaging whole bodies but with much lower spatial resolution. The combination of MRI with luminescence imaging methods using a single molecule is appealing as such a probe would combine the broad scope of MRI with the fine detail allowed by luminescence imaging.[5]

This possibility has stimulated interest in a range of heteronuclear d/f complexes in which one or more phosphorescent d-block units is connected to one or more stable Gd(III) units. Notable recent examples have come from the groups of Faulkner[6] and Parac-Vogt[7] amongst others.[5,8] A common feature of these is that the Gd(III) unit is coordinated by a saturated poly-amino/carboxylate ligand of the 'DTPA' or 'DOTA' types as these provide the necessary high kinetic and thermodynamic stability in aqueous media. A disadvantage of these however is that the saturated skeletons can permit free rotation of the Gd(III) unit independently of the rest of the molecule, which limits relaxivity: high relaxivities arise from slow molecular tumbling in solution which gives long rotational correlation times, and many synthetic strategies have been employed specifically to rigidify Gd(III) complexes to increase their relaxivity.[4,5]

We report here a new ligand architecture (Fig. 1), which allows a strongly phosphorescent Ir(III) unit to be connected to a water-stable Gd(III) unit *via* a fully conjugated and rigid connector. This results in both (i) long-lived luminescence which can be used in PLIM imaging under one-photon or two-photon excitation, and (ii) unusually long relaxivity from a single Gd(III) centre as a consequence of the rigid design. The combination of Ir(III) and Gd(III) components for dual-imaging purposes has been very little explored[8c] and this report is the first demonstration of PLIM using a complex that also has high relaxivity for MRI purposes. As an additional benefit, the same ligand architecture provides an effective through-bond coupling pathway for efficient Dexter Ir(III)→Eu(III) energy-transfer (EnT) in the isostructural **Ir•Eu** complex. Dual-luminescent d/f complexes are of interest for a range of applications from imaging[9] to white-light emission[10] and many of these applications hinge on the extent of d→f EnT which controls the balance of luminescence output from the two components.[11,12] We prepared **Ir•Eu** as an adjunct to **Ir•Gd** to allow measurement of the q value around the Ln(III) centre, but its properties arising from the ligand structure are of significant interest in their own right.

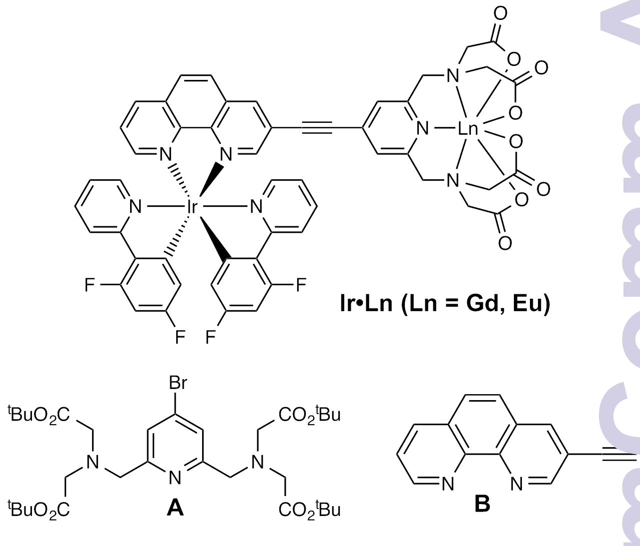

Fig. 1 Structural formulae of the complexes **Ir•Ln** and of the starting materials **A** and **B** (see ESI for full synthetic scheme).

The complexes **Ir•Ln** [where Ln = Gd(III) and Eu(III) respectively] are shown in Fig. 1. The Ir(III) unit is one of the well-known $\{Ir(F_2phpy)_2(NN)\}^+$ units based on cyclometallating fluorinated phenyl-pyridine ligands.[13] The Gd(III) coordination is provided by a heptadentate pyridine-2,6-bis(amino-diacetate) chelating unit,[14] connected to the $\{Ir(F_2ppy)_2(phen)\}^+$ chromophore *via* an alkynyl linkage, providing the rigid, fully conjugated pathway containing no sp^3-hybridised atoms. The key step is a Sonogashira coupling reaction between compounds **A** (the 4-bromopyridine with two pendant, protected, amino-diacetate arms) and 3-ethynyl-1,10-phenanthroline (**B**). After assembling the ligand skeleton, coordination of the phen to an $\{Ir(F_2ppy)_2\}^+$ unit, unmasking of the amino/carboxylate binding site by removal of the esters, and finally incorporation of Ln(III), all used standard methods (see ESI); the final products **Ir•Ln** were purified by HPLC and characterised by mass spectrometry and elemental analysis.

The UV/Vis absorption spectra of **Ir•A** [the free tetracarboxylic acid complex with no Gd(III)] and **Ir•Ln** show the usual intense absorptions in the visible region associated with ligand-centred $\pi\rightarrow\pi^*$ transitions (see Fig. S14, ESI). In addition the weak shoulder and long tail between 400 nm to 550 nm is ascribed to the Ir(III)→phen MLCT transition.[13] The luminescence of **Ir•A** at 530 nm, and **Ir•Gd** at 560 nm, are broad and featureless, indicative of ^{3}MLCT luminescence (Fig. 2a): the red-shift in **Ir•Gd** may be ascribed to the effect of the Gd(III) ion whose positive charge stabilises the LUMO of the conjugated phen/alkyne/pyridyl ligand. Assignment of the luminescence as ^{3}MLCT is supported by the substantial rigidichromism: at 77K (MeOH/EtOH glass) the highest-energy feature in the luminescence spectrum of **Ir•Gd** (which now shows a clear sequence of vibronic components, Fig. 2a) is blue-shifted from 560 nm to 495 nm, giving an energy of 20200 cm^{-1} for the Ir(III)-based ^{3}MLCT excited state. In aqueous solution at RT the Ir(III)-based emission of **Ir•Gd** (ϕ = 4%) shows two decay components with lifetimes of τ_1:1100 ns (56%) and τ_2:450 ns (44%). The presence of two components is a common consequence of aggregation in solution,[12a,12b] possibly associated with the hydrophobic $\{Ir(F_2\text{-}phpy)(phen)\}^+$ units.

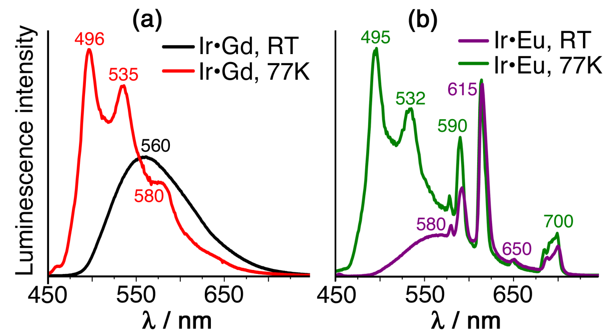

Fig. 2 Luminescence spectra in MeOH/EtOH (1:4) of (a) **Ir•Gd**, in fluid solution at RT (black) and as a frozen glass at 77K (red); and (b) **Ir•Eu** in fluid solution at RT (purple) and as a frozen glass at 77K (green). λ_{ex} = 400 nm in all cases.

The luminescence properties of **Ir•Eu** are also of interest. The ^{3}MLCT excited-state energy of the Ir(III)-component at 20,200 cm^{-1} is sufficient to allow sensitisation of the Eu(III) $^5D_0$ state which lies at *ca.* 17,500 cm^{-1}; at RT a gradient for EnT between donor (Ir) and acceptor (Eu) of *ca.* 2000 cm^{-1} is required.[15] The luminescence spectrum of **Ir•Eu** in solution shows how partial Ir(III)→Eu(III) EnT has occurred, with the Ir(III)-based luminescence reduced in intensity by 22 % compared to what was observed for **Ir•Gd**, and five sharp luminescence lines at 580, 590, 615, 687 and 700 nm from the Eu(III) $^5D_0\rightarrow{}^7D_n$ transitions superimposed on the low-energy tail of the Ir(III)-based luminescence making it appear red (Fig. S13, ESI). At 77K the two emission components are more clearly separated because of the rigidochromic blue-shift of the Ir(III)-based emission component (Fig. 2b).

The Ir(III)→Eu(III) EnT reduces the Ir(III)-based luminescence lifetime (compared to **Ir•Gd**) to τ_1 = 780 and τ_2 = 116 ns (again, we see two components). If we make the reasonable assumption that Ir(III)→Eu(III) EnT provides the best additional deactivation pathway for Ir(III)-based luminescence in **Ir•Eu** compared to what is possible in **Ir•Gd**, then the shortest luminescence component of 116 ns in **Ir•Eu** is associated with intramolecular quenching by Ir(III)→Eu(III) EnT. This gives from eq. 1 (where τ_u is the 'unquenched' lifetime from **Ir•Gd** and τ_q is the 'quenched' lifetime from **Ir•Eu**) an EnT rate k_{EnT} of *ca.* 6×10^6 sec^{-1}. Significantly this is an order of magnitude faster than we observed in our previous 'rod-like' water-soluble Ir(III)–Eu(III) dyad that was investigated for cell imaging, despite the greater Ir•••Eu separation. The markedly supirior Ir(III)→Eu(III) EnT in **Ir•Eu** can be ascribed to the fully conjugated pathway facilitating Dexter energy-transfer[12] in this present system. All the photophysical results are summarised in Table S1 in ESI.

$$k_{EnT} = 1/\tau_q - 1/\tau_u \qquad (1)$$

To assess the suitability of the complexes as probes for PLIM imaging, their cellular localization, emission properties and toxicity were evaluated in live MCF7 cells. Cells were incubated with **Ir•Ln** at 25 μM, 50 μM and 100 μM for 4 and 24 hours in fully supplemented Roswell Park Memorial Institute (RPMI) media at 37°C. Steady-state confocal microscopy (typical images in Fig. 3a), shows that **Ir•Gd** exhibits punctate cytoplasmic staining with some accumulation in the perinuclear region, the latter being most notable at high concentrations and long incubation times. Ir(III)-based emission was observed under both one-photon (458 nm) and two-photon (780 nm) excitation, consistent with the known modest two-photon absorption ability of Ir(III) complexes of this family.[9,16] Optical sectioning (Fig. S21, ESI) and co-staining with the commercial nuclear stain DAPI (Fig. S22, ESI) confirm that **Ir•Gd** was internalized into the cell cytoplasm, but did not cross the nuclear membrane.

Interestingly, **Ir•Gd** appeared to be internalized more rapidly than the isostructural **Ir•Eu** complex. Fig. 3b shows steady-state confocal images after 24 hours incubation at 100 μM, recorded with the same laser power and detector gain. Emission from **Ir•Gd** incubated cells is significantly brighter than that of **Ir•Eu**, to the extent that the detail of the staining pattern cannot be clearly distinguished (due to the high detector gain). This difference is not solely due to the inherently brighter Ir(III)-based emission in **Ir•Gd**. The significant effect **Ir•Gd** has on the metabolic activity of MCF cells in comparison to **Ir•Eu** suggest that considerably more **Ir•Gd** is taken up by the cells (see Fig. S 23). The reason for this difference in uptake between **Ir•Gd** and **Ir•Eu** is not obvious but the effect is clear, with lower concentrations / shorter incubation times being typically preferred for **Ir•Gd**.

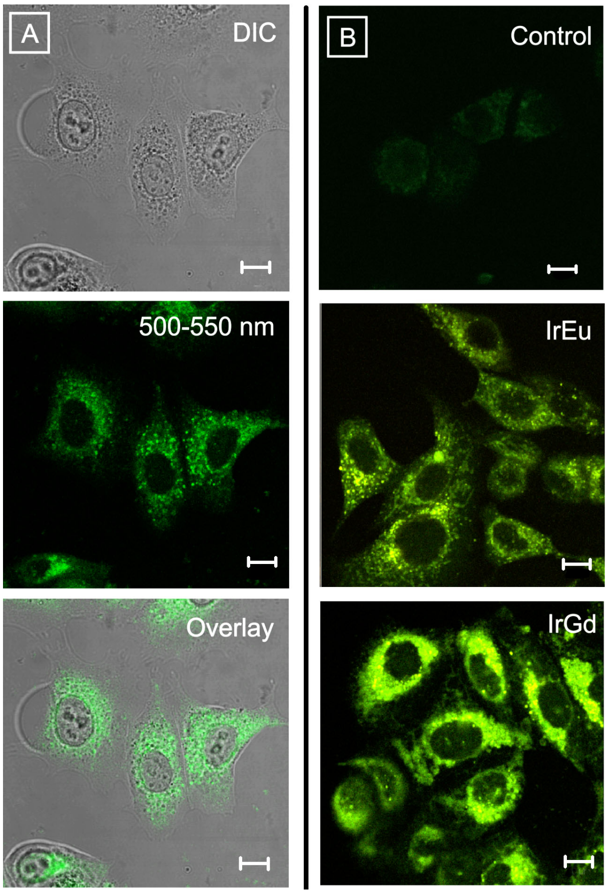

Fig. 3 Two-photon (λ_{ex} = 780 nm) steady-state confocal imaging of **Ir•Ln** complexes. Column (A), in descending order: DIC, emission and overlay images showing typical staining pattern of **Ir•Ln** dyads in live MCF7 cells (**Ir•Gd**, 50 µM, 4h). Column (B): cellular uptake comparison after 24 hour incubation with (in descending order): RPMI media only, **Ir•Eu** (100 µM), **Ir•Gd** (100 µM).

Lifetime mapping of the Ir(III)-based emission from both dyads was carried out using TP-PLIM (Fig. 4). In both cases, emission decays were best fit to a double exponential and only the major component (>86%) τ_1 was used for plotting lifetime maps. The Ir(III)-based luminescence lifetimes are uniform across the cells for both dyads, with the lifetime values being comparable to those observed in aerated solution. Fig. 4 also highlights the clear difference in Ir(III)-based luminescence lifetimes between **Ir•Gd** and **Ir•Eu**, brought about by energy transfer, by showing both lifetime maps set to the same parameters (rainbow chart = 0 – 600 ns). **Ir•Gd** appears green (longer lifetime), whereas **Ir•Eu** appears orange due a shorter lifetime. Example decay traces for each dyad were exported and overlaid for comparison (Fig. 4).

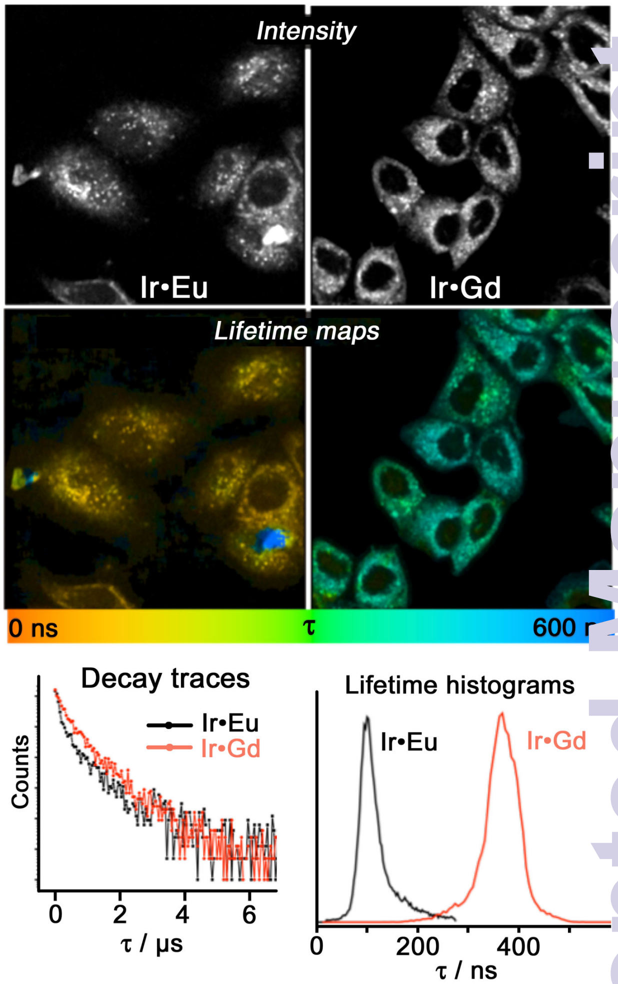

Fig. 4 Two-photon PLIM imaging (λ_{ex} = 780 nm, 12 µs imaging window of **Ir•Eu** (100 µM, 20 h) and **Ir•Gd** (25 µM, 20 h) in live MCF7 cells. **Top**: Intensity images, where all emitted photons are binned into on channel. **Middle**: τ_1 lifetime maps with rainbow legend set to 0 – 600 n for both images, showing unifomity of cellular lifetime for each compound and the difference in Ir(III)-based emission lifetime betwe **Ir•Eu** and **Ir•Gd**. **Bottom**: emission decay traces and lifet dsitributions of the Ir(III)-based emission from **Ir•Gd** and **Ir•Eu** in the cells.

From **Ir•Eu** we found that the Eu(III)-based luminescenc lifetimes were 0.42 ns in water and 1.14 ms in D_2O, giving value for *q* of 1.6 ± 0.5,[17] comparable to what is observed with other Gd(III) complexes of heptadentate ligands used for MRI.[4] Despite this, at 20 MHz and 37°C the relaxivity of **Ir•Gd** is 11. mM^{-1} s^{-1}, measured over a range of concentrations (see ESI). This is considerably higher than that of typical mononuclear Gd(III) complexes (typically, 4 – 5 mM^{-1} s^{-1})[4,5] and must be consequence of the rigidity imposed on the complex by the conjugated linkage. Notably, this is comparable to relaxivity values observed in other d/f hybrids which contain three or f Gd(III) centres that are individually more flexible due to the saturated ligand skeletons.[5c] Thus the ligand design in **Ir•Gd** is clearly effective at providing high relaxivity for a relatively low molecular weight complex without the need to incorporate several Gd(III) centres, or to conjugate the probe to biomolecule to slow down its rotational correlation time.

For imaging purposes with Ln(III)-containing complexes, kinetic stability is important due to the toxicity of free Ln(III) ions. The luminescence spectra of **Ir•Gd** and **Ir•Eu** showed no change after prolonged storage in aqueous solution: loss of the Ln(III) ion would result in each case in a blue shift of the Ir(III)-based emission maximum from 564 nm to 532 nm due to the generation of free **Ir•A** (Fig. S15). In addition, the kinetic stability of **Ir•Eu** was measured by luminescence spectroscopy in the presence of 1 equivalent of the competing ligand DOTA [the octadentate macrocyclic ligand system cyclen-1,4,7,10-tetraacetic acid, used as a Ln(III) receptor] at a concentration of 0.1 mM, in both water and in PBS buffer (see Fig. S19 and Fig. S20 respectively). If the Eu(III) ion were extracted from **Ir•Eu** by the competing DOTA ligand, we would see a steady loss of sensitised Eu(III)-based luminescence as well as the blue-shift of the Ir(III)-based emission component. In the presence of DOTA, the Ir(III)-based emission showed no significant change in profile, and the sensitised Eu(III)-based luminescence remained almost intact (<5% decrease in intensity after 3 days), confirming the integrity of the complex even under these challenging conditions (Fig. S19). When PBS buffer was used as the medium, greater loss of Eu-based luminescence intensity was observed (Fig. S20) presumably associated with the presence of phosphate.

In conclusion, this ligand architecture offers substantial scope for dual (luminescence + magnetic resonance) imaging using d/f complexes because of its rigidity; and for applications requiring d→f energy-transfer because of the conjugated pathway. Thus **Ir•Gd** provides both the capacity for PLIM measurements as well as unusually high relaxivity for a mononuclear Gd(III) complex; and **Ir•Eu** demonstrates unusually effective d→f Dexter energy-transfer.

We thank the European Commission for a Marie-Curie fellowship to A. J.

Notes and references

[a] *Department of Chemistry, University of Sheffield, Sheffield S3 7HF, UK. E-mail: m.d.ward@sheffield.ac.uk*
[b] *School of Chemistry, Cardiff University, Main building, Park Place, Cardiff CF10 3AT.*

† Electronic Supplementary Information (ESI) available: Detailing the synthesis of both **Ir•Ln** complexes, cell culture and staining, toxicity testing and PLIM iamging. ^{1}H and ^{13}C NMR, mass spectra, HPLC traces are included along with additional UV-vis absorption and luminesnce spectra, confocal, PLIM and MRI images. See DOI: 10.1039/b000000x/

1 Reviews: (a) J.-C. G. Bünzli, *Chem. Rev*., 2010, **110**, 2729; (b) E. J. New, D. Parker, D. G. Smith and J. W. Walton, *Curr. Opin. Chem. Biol*., 2010, **14**, 238; (c) Q. Zhao, C. Huang and F. Li, *Chem. Soc. Rev*., 2011, **40**, 2508; (d) E. Baggaley, J. A. Weinstein and J. A. G. Williams, *Coord. Chem. Rev*., 2012, **256**, 1762; (e) Y. You, *Curr. Opin. Chem. Biol*., 2013, **17**, 699; (f) M. P. Coogan and V. Fernández-Moreira, *Chem. Commun*., 2014, **50**, 384; (g) K. K.-W. Lo and S. P.-Y. Li, *RSC Adv*., 2014, **4**, 10560.

2 Illustrative recent examples: (a) S. W. Botchway, M. Charnley, J. W. Haycock, A. W. Parker, D. L. Rochester, J. A. Weinstein and J. A. G. Williams, *Proc. Natl. Acad. Sci. USA,* 2008, **105**, 16071; (b) V. Fernández-Moreira, M. L. Ortego, C. F. Williams, M. P. Coogan, M. D. Villacampa and M. C. Gimeno, *Organometallics,* 2012, **31**, 5950; (c) G. Li, Y. Chen, J. Wu, L. Ji and H. Chao, *Chem. Commun*., 2013, **49**, 2040; (d) E. Baggaley, M. R. Gill, N. H. Green, D. Turton, I. V. Sazanovich, S. W. Botchway, C. Smythe, J. W. Haycock, J. A. Weinstein and J. A. Thomas, *Angew. Chem., Int. Ed.,* 2014, **53**, 3367; (e) S. J. Butler, L. Lamarque, R. Pal and D. Parker, *Chem. Sci*., 2014, **5**, 1750.

3 (a) R. I. Dmitriev, A. V. Zhdanov, Y. M. Nolan and D. B. Papkovsky, *Biomaterials,* 2013, **34**, 9307; (b) E. Baggaley, J. A. Weinstein and J. A. G. Williams, *Struct. Bonding (Springer)*, 2014, **168**, 1; (c) E. Baggaley, S. W. Botchway, J. W. Haycock, H. Morris, I. V. Sazanovich, J. A. G. Williams and J. A. Weinstein, *Chem. Sci.,* 2014, **5**, 879; (d) E. Baggaley, I. V. Sazanovich, J. A. G. Williams, J. W. Haycock, S. W. Botchway and J. A. Weinstein, *RSC Adv.,* 2014, **4**, 35003; (e) R. I. Dmitriev, A. V. Kondrashina, K. Koren, I. Klimant, A. V. Zhdanov, J. M. P. Pakan, K. W. McDermott and D. B. Papkovsky, *Biomaterials Science,* 2014, **2**, 853.

4 (a) P. Caravan, J. J. Ellison, T. J. McMurry and R. B. Lauffer, *Chem. Rev.,* 1999, **99**, 2293; (b) É. Tóth, L. Helm and A. E. Merbach, in *Comprehensive Coordination Chemistry, Vol. 9* (Ed. M. D. Ward), Elsevier, 2004: Chapter 19, pp 841–881; (c) S. Aime, A. Barge, E. Gianolio, R. Padliarin, L. Silengo and L. Tei, in *Molecular Imaging: An Essential Tool in Preclinical Research, Diganostic Imaging, and Therapy*, (Eds. A. A. Bogdanov, K. Licha), Springer, 2005: Chapter 6, pp 99–121.

5 (a) L. E. Jennings and N. J. Long, *Chem. Commun.,* 2009, 3511 and refs. therein; (b) C. S. Bonnet and É. Tóth, *Comptes Rend. Chim.,* 2010, **13**, 700 and refs. therein; (c) E. Debroye and T. N. Parac-Vogt, *Chem. Soc. Rev.,* 2014, **43**, 8178 and refs. therein.

6 (a) T. Koullourou, L. S. Natrajan, H. Bhavsar, S. J. A. Pope, J. H. Feng, J. Narvainen, R. Shaw, E. Scales, R. Kauppinen, A. M. Kenwright and S. Faulkner, *J. Am. Chem. Soc.,* 2008, **130**, 2178; (b) M. Tropiano, C. J. Record, E. Morris, H. S. Rai, C. Allain and S. Faulkner, *Organometallics,* 2012, **31**, 5673.

7 (a) P. Verwilst, S. V. Eliseeva, L. Vander Elst, C. Burtea, S. Laurent, S. Petoud, R. N. Muller, T. N. Parac-Vogt and W. M. De Borggraeve, *Inorg. Chem.,* 2012, **51**, 6405; (b) G. Dehaen, S. V. Eliseeva, K. Kimpe, S. Laurent, L. Vander Elst, R. N. Muller, W. Dehaen, K. Binnemans and T. N. Parac-Vogt, *Chem. Eur. J.,* 2012, **18**, 293.

8 (a) J. Luo, W.-S. Li, P. Xu, L.-Y. Zhang and Z.-N. Chen, *Inorg. Chem.,* 2012, **51**, 9508; (b) X. Zhang, X. Jing, T. Liu, G. Han, H. Li and C. Duan, *Inorg. Chem.,* 2012, **51**, 2325; (c) H. Yang, L. Ding, L. An, Z. Xiang, M. Chen, J. Zhou, F. Li, D. Wu and S. Yang, *Biomaterials,* 2012, **13**, 8591; (d) J. Luo, L.-F. Chen, P. Hu and Z.-N. Chen, *Inorg. Chem.,* 2014, **53**, 4184.

9 E. Baggaley, D.-K. Cao, D. Sykes, S. W. Botchway, J. A. Weinstein and M. D. Ward, *Chem. Eur. J.,* 2014, **20**, 8898.

10 P. Coppo, M. Duati, V. N. Kozhevnikov, J. W. Hofstraat and L. De Cola, *Angew. Chem., Int. Ed.,* 2005, **44**, 1806.

11 M. D. Ward, *Coord. Chem. Rev.,* 2010, **254**, 2634.

12 (a) T. Lazarides, D. Sykes, S. Faulkner, A. Barbieri and M. D. Ward, *Chem. Eur. J.,* 2008, **14**, 9389; (b) D. Sykes, I. S. Tidmarsh, A. Barbieri, I. V. Sazanovich, J. A. Weinstein and M. D. Ward, *Inorg. Chem*., 2011, **50**, 11323; (c) D. Sykes, S. C. Parker, I. V. Sazanovich, A. Stephenson, J. A. Weinstein and M. D. Ward, *Inorg. Chem*., 2013, **52**, 10500.

13 L. Flamigni, A. Barbieri, C. Sabatini, B. Ventura and F. Barigelletti, *Top. Curr. Chem.,* 2007, **281**, 143.

14 V.-M. Mukkala, C. Sund, M. Kwiatkowski, P. Pasanen, M. Högberg, J. Kankare and H. Takkalo, *Helv. Chim. Acta,* 1992, **75**, 1621.

15 (a) S. Sato and M. Wada, *Bull. Chem. Soc. Jpn.,* 1970, **43**, 1955; (b) D. Parker, *Coord. Chem. Rev.,* 2000, **205**, 109.

16 (a) L. S. Natrajan, A. Toulmin, A. Chew and S. W. Magennis, *Dalton Trans.,* 2010, **39**, 10837; (b) R. M. Edkins, S. L. Bettington, A. E. Goeta and A Beeby, *Dalton Trans.,* 2011, **40**, 12765; (c) M.-L. Ho, M.-H. Lin, Y.-T. Chen and H.-S. Sheu, *Chem. Phys. Lett.,* 2011, **509**, 162; (d) W.-J. Xu, S.-J. Liu, X. Zhao, N. Zhao, Z.-Q. Liu, H. Xu, H. Liang, Q. Zhao, X.-Q. Yu and W. Huang, *Chem. Eur. J.,* 2013, **19**, 621.

17 A. Beeby, I. M. Clarkson, R. S. Dickins, S. Faulkner, D. Parker, L. Royle, A. S. de Sousa, J. A. G. Williams and M. Woods, *J. Chem. Soc., Perkin Trans. 2*, 1999, 493.